iScience

CellPress
OPEN ACCESS

Article

# Development of OX40 agonists for canine cancer immunotherapy

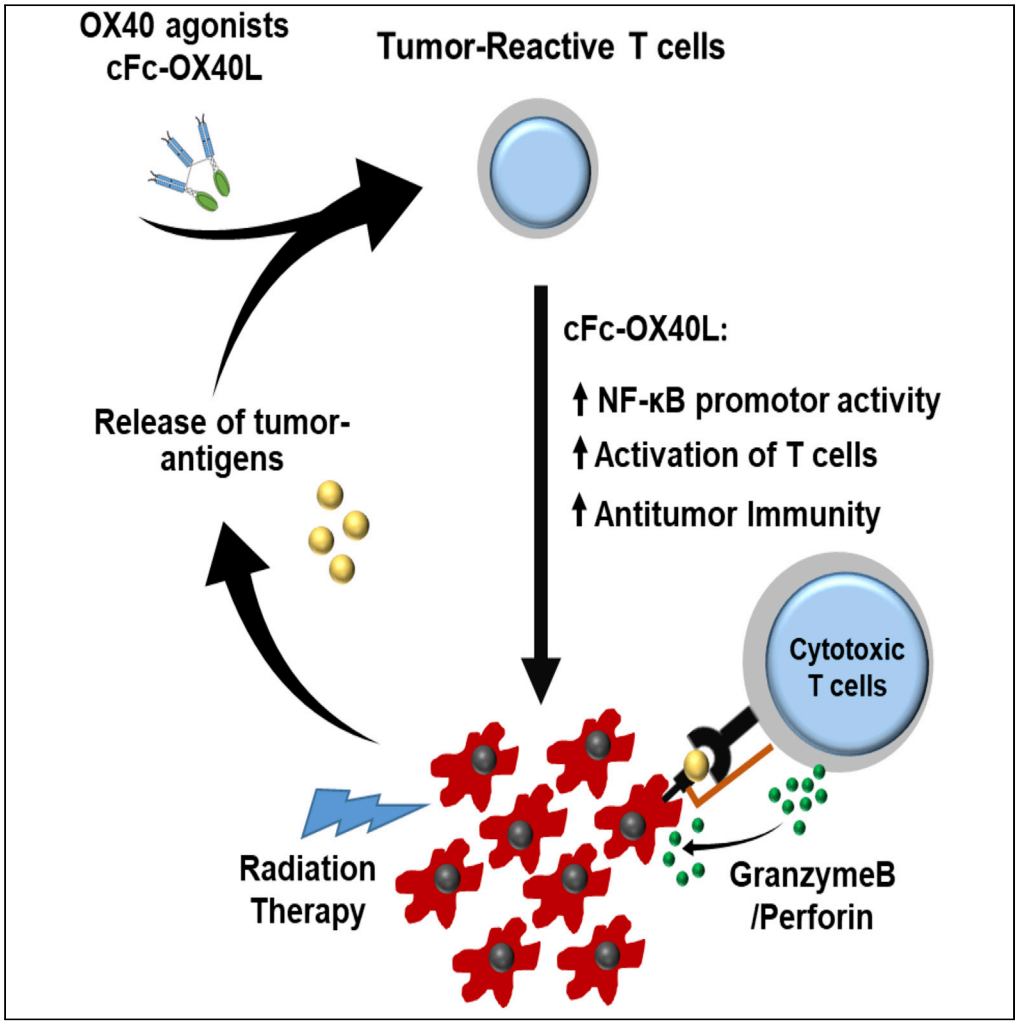


Damien Ruiz, Chloe Haynes, Jonathan Marable, ..., Amarjit Mishra, Bruce F. Smith, Maninder Sandey

mzs0011@auburn.edu

## Highlights

Canine FcOX40L recombinant proteins act as potent OX40 agonists

cFcOX40L induces NF-κB signaling and IFN-γ secretion from activated cPBMCs

cOX40 is expressed at high levels on TILs in canine osteosarcoma (OS)

Ruiz et al., iScience 25, 105158
October 21, 2022 
https://doi.org/10.1016/j.isci.2022.105158

iScience

CellPress
OPEN ACCESS

Article

# Development of OX40 agonists for canine cancer immunotherapy

Damien Ruiz,[1] Chloe Haynes,[1] Jonathan Marable,[1] Chetan Pundkar,[1] Rebecca L. Nance,[2] Deepa Bedi,[3] Payal Agarwal,[1,2] Amol S. Suryawanshi,[1] Amarjit Mishra,[1] Bruce F. Smith,[1,2] and Maninder Sandey[1,4,*]

## SUMMARY

**Recent breakthroughs in cancer immunotherapy have provided unprecedented clinical benefits to human cancer patients. Cancer is also one of the most common causes of death in pet dogs. Thus, canine-specific immune therapies targeting similar signaling pathways can provide better treatment options for canine cancer patients. Here, we describe the development and characterization of two canine-specific anti-OX40 agonists to activate OX40 signaling. We show that canine OX40, like human OX40, is not expressed on resting T cells, and its expression is markedly increased on canine CD4 T cells and Tregs after stimulation with concanavalin A (Con-A). cOX40 is also expressed on tumor-infiltrating lymphocytes (TILs) in canine osteosarcoma patients. The canine-specific OX40 agonists strongly activates cPBMCs by increasing IFN-γ expression and do not require Fc receptor-mediated cross-linking for OX40 agonism. Together, these results suggest that cFcOX40L proteins are potent OX40 agonists and have the potential to enhance antitumor immunity in canine cancer patients.**

## INTRODUCTION

Cancer is the leading cause of death in dogs over ten years of age (Adams et al., 2010; Fleming et al., 2011). Current treatment options, including surgery, radiation therapy, and chemotherapy, provide limited clinical benefits. Over the past few years, immune checkpoint inhibitors (ICIs) have profoundly improved the management of several advanced malignancies in humans (Diamantopoulos and Gogas, 2016; Cloughesy et al., 2019; Wolchok et al., 2013; Alsaab et al., 2017). ICIs bind and block inhibitory immune checkpoint molecules such as programmed cell death receptor-1 (PD-1), its receptor (PD-L1), and cytotoxic T lymphocyte-associated antigen-4 (CTLA-4) to overcome tumor-mediated inhibition of T cell function, leading to the reinvigoration of antitumor immune response (Buchbinder and Desai, 2016; Diamantopoulos and Gogas, 2016; Cloughesy et al., 2019; Wolchok et al., 2013; Alsaab et al., 2017). Several studies are currently developing or investigating canine-specific ICIs to provide similar clinical benefits to canine cancer patients (Igase et al., 2020; Mason et al., 2021; Marable et al., 2021). In an alternative approach, various costimulatory molecules, including OX40 (CD134), glucocorticoid-induced TNFR (GITR, CD357), and 4-1BB (CD137), can be targeted to augment T cell immunity in tumor-bearing hosts (Bartkowiak and Curran, 2015; Melero et al., 2013; Chan et al., 2022; Gutierrez et al., 2021).

The engagement of the TNF superfamily of ligands (TNFSF) and receptors (TNFRSF) is critical for the differentiation of naive lymphocytes into antigen-specific CD4 and CD8 T cells (Gramaglia et al., 1998; Huddleston et al., 2006). OX40, a member of the TNFRSF, is vital in activating, expanding, and survival of antigen-specific T-cells (Gramaglia et al., 1998; Huddleston et al., 2006). OX40, along with CD28, is responsible for clonal expansion of antigen-reactive CD4 naive T cells (Redmond et al., 2009; Song et al., 2005). Working with OX40-deficient mice has clearly demonstrated the central role of OX40 in initiating the antigen-specific immune response (Kopf et al., 1999). Compared to wild-type, the OX40 knockout mice develop very few primary effector CD4 & CD8 T cells after immunization (Gaspal et al., 2005; Kopf et al., 1999). Moreover, these mice also have a low number of memory CD4 T cells. OX40 signals also block the suppressing ability of natural regulatory T cells (Tregs) and prevent the generation of inducible Tregs (Gramaglia et al., 2000; Vu et al., 2007; Rogers et al., 2001).

OX40 is not expressed on naive lymphocytes in humans; however, its expression is rapidly upregulated on CD4 and CD8 T cells following T cell receptor (TCR) ligation. Similarly, the expression of its

[1]Department of Pathobiology, College of Veterinary Medicine, Auburn University, Auburn, AL, USA

[2]Scott Ritchy Research Center, College of Veterinary Medicine, Auburn University, Auburn, AL, USA

[3]Biomedical Sciences, Tuskegee University, Tuskegee, AL, USA

[4]Lead contact

*Correspondence: mzs0011@auburn.edu

https://doi.org/10.1016/j.isci.2022.105158

ligand, OX40L, is also upregulated on activated antigen-presenting cells (APCs) such as dendritic cells, B cells, and macrophages (Gramaglia et al., 1998). OX40 is a type-I transmembrane protein with an N-terminus extracellular receptor-binding domain (RBD), while OX40L is a type-II transmembrane protein with an extracellular domain (ECD) on its C-terminus (Compaan and Hymowitz, 2006). OX40L contains a TNF homology domain (THD) in its ECD that interacts with similar domains from other protomers to form non-covalent bonded homotrimers (Vanamee and Faustman, 2018; Compaan and Hymowitz, 2006). When OX40L engages OX40, the receptor trimerizes and initiates a signaling cascade that activates PI3K (PI-3-kinase)/PKB (protein kinase B/Akt) and NF-κB1 pathways (Rogers et al., 2001). Activation of these pathways causes up-regulation of several anti-apoptotic Bcl-2 family members, including Bcl-xL, Bcl-2, and Bfl-1, and molecules that regulate cell division such as survivin and aurora B kinase (Croft et al., 2009; Rogers et al., 2001).

OX40L mediated trimerization is crucial for activating OX40 signaling (Bodmer et al., 2002; Compaan and Hymowitz, 2006). Thus, when designing an optimal therapeutic OX40 agonist, recapitulating these inherent physical characteristics is essential (Mayes et al., 2018). As mAbs are bivalent, anti-OX40 mAbs are dependent on the interaction between the Fc region and Fcγ receptors (FcγR) for OX40 activation (Chen et al., 2019; Glisson et al., 2020). Alternatively, self-trimerizing Fc-OX40L fusion proteins could be engineered to activate the OX40 signaling. In Fc-OX40L fusion proteins, the ECD of OX40L is fused to the Fc domain of human IgG via a coiled-coil trimerization domain (Morris et al., 2007). These fusion proteins naturally form hexamers and do not require Fcγ receptor-mediated cross-linking for OX40 agonism (Morris et al., 2007).

Several preclinical studies have investigated the antitumor activity of Fc-OX40L fusion protein and anti-OX40 mAbs in mouse tumor xenograft models of various human cancers, including melanoma, breast cancer, sarcomas, and colon cancers (Burocchi et al., 2011; Hirschhorn-Cymerman et al., 2012; Murata et al., 2006; Murphy et al., 2014; Pardee et al., 2010; Piconese et al., 2008). Anti-OX40 agonist mAbs or OX40L-Fc fusion proteins cause expansion of tumor-reactive CD4 and CD8 T cells and deplete Tregs from the tumor microenvironment (TME), resulting in tumor regression and survival benefits (Burocchi et al., 2011; Hirschhorn-Cymerman et al., 2012; Murata et al., 2006; Murphy et al., 2014; Pardee et al., 2010; Piconese et al., 2008). Moreover, combination immunotherapy with anti-OX40/anti-CTLA-4 or anti-OX40/anti-PD1 mAbs dramatically improves survival in poorly immunogenic TRAMP-C1 prostate, PDAC pancreatic cancer, and MCA-205 sarcoma xenograft models (Guo et al., 2014; Lee et al., 2004; Redmond et al., 2014; Smith et al., 2011). Currently, several clinical trials are investigating the antitumor activity of anti-OX40 mAbs either as monotherapy or in combination with ICIs in human cancer patients (Glisson et al., 2020). The preliminary results from these studies show that anti-OX40 mAbs increase the number of tumor-specific CD4 and CD8 T cells (Duhen et al., 2021).

Here, we characterize the genomic location, structural properties, and expression profile of canine orthologs of OX40/OX40L. We also engineered two canine-specific cFcOX40L fusion proteins as OX40 agonists. We show that both cFcOX40L fusion proteins are potent OX40 agonists and induce NF-κB promoter activity in OX40-effector cells. We also show that canine OX40, like humans, is also expressed on tumor-infiltrating lymphocytes (TILs). We also confirmed the ability of cFcOX40L fusion proteins to activate and induce the expression of IFN-γ from canine peripheral blood mononuclear cells (cPBMCs).

## RESULTS

### Canine OX40 shares high sequence similarity to human ortholog

We used a predicted mRNA sequence (Genebank: XM_038664292) from the National Center for Biotechnology Information (NCBI) database to amplify the open reading frame (ORF) of canine OX40. The canine (c)OX40 ORF was successfully amplified and sequenced from canine peripheral blood mononuclear cells (cPBMCs). The amplified DNA sequence was 100% similar to the predicted mRNA sequence. The canine OX40 locus is located on chromosome 5, and the ORF is derived from 7 exons that vary in size from 67 bps to 299 bps. The canine OX40 protein consists of 273 amino acids. It has the typical type I transmembrane protein structure with an extracellular domain of 218 amino acids, a transmembrane region of 22 amino acids, and a cytoplasmic domain of 33 amino acids. The signal secretion peptide was predicted to be 28 aminoacid long with a cleavage site between the $28^{th}$ and $29^{th}$ amino acids (98% probability with SignalP 6.0 software analysis). Canine OX40 displays an overall identity of about 67% to the human ortholog (Figures 1A and 1B). The canine OX40 protein has 18 conserved cysteine residues in the ectodomain

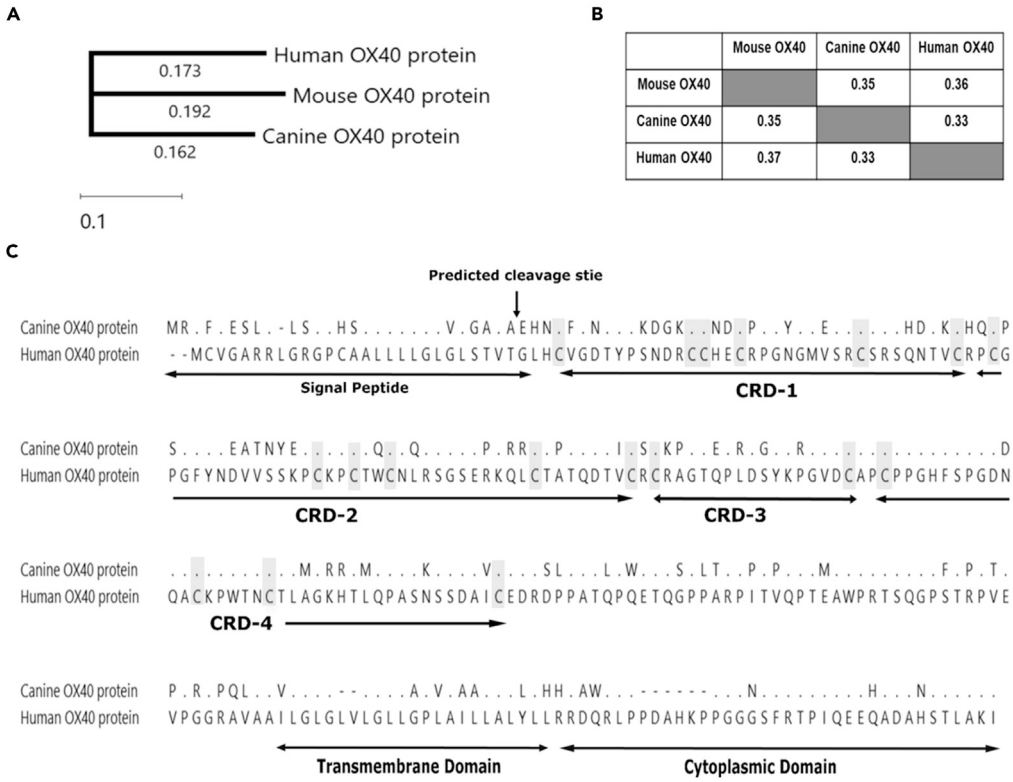


**Figure 1. Comparison of OX40 structure**

(A) Phylogenetic analysis of OX40 proteins.

(B) Aminoacid similarity between canine, mouse, and human OX40.

(C) Aminoacid alignment of OX40. Extracellular, Transmembrane, and cytoplasmic domains are indicated. Gray boxes highlight the conserved cysteine residues. The signal secretion peptide is 28 amino acids long, and the cleavage site is between the 28$^{th}$ and 29$^{th}$ amino acids. CRD-Cysteine Rich Domain.

that form nine disulfide bonds in CRD1, CRD2, CRD3, and CRD4 domains (Figure 1C). Collectively, our data show that cOX40 has a highly similar structure to its human ortholog.

## Canine OX40 ligand shares characteristic structural features with its human ortholog

Our next goal was to identify and amplify the sequence of canine OX40 ligand (OX40L). The predicted mRNA sequence (Genebank: XM_003639167) of the canine OX40 ligand was retrieved from the NCBI database. The canine OX40L locus was located on chromosome 7, and the ORF is derived from three exons that vary in size from 48 to 3043 bps. The OX40L mRNA contains a long 3'untranslated region (UTR). The canine OX40L protein consists of 183 amino acids and has an overall identity of about 68% to its human ortholog (Figures 2A and 2B). The extracellular domain of the canine OX40L ligand has F180 and N166 amino acids in the C-terminal extension and H strand, two critical residues that make a significant contribution in binding to OX40 (Figure 2C). Thus, like cOX40, cOX40L also has a very similar structure to human OX40L.

## Production and characterization of cFcOX40L$_B$

The structure of the cFcOX40L$_B$ fusion protein was constructed based on human Fc-OX40L (Morris et al., 2007). To build cFcOX40L$_B$, we used the Fc region of subclass B of the canine IgG (functional analog of human IgG1). The recombinant cFcOX40L$_B$ was actively secreted into the conditioned media and expressed at high levels by transiently transfected ExpiCHO-S cells (Figure 3A). Western blot analysis showed that the cFcOX40L$_B$ was present predominantly as monomers under reducing conditions with a molecular weight (MW) of 51 kDa. It forms dimers with an MW of 102 kDa under non-denaturing conditions (Figure 3A). The cFcOX40L$_B$ was successfully purified by affinity (protein A) and size-exclusion chromatography (Figure 3B). To characterize the binding of cFcOX40L$_B$ to canine OX40, we successfully amplified and cloned the ORF coding for canine OX40 into the pCDNA3.1$^+$/Hygro vector. This

A

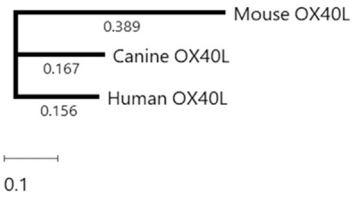


B

| | Mouse OX40L | Canine OX40L | Human OX40L |
|---|---|---|---|
| Mouse OX40L | | 0.56 | 0.54 |
| Canine OX40L | 0.56 | | 0.32 |
| Human OX40L | 0.54 | 0.32 | |

C

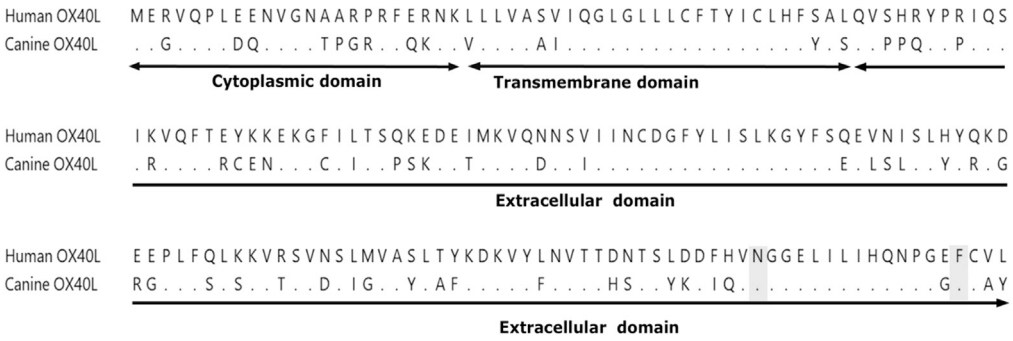


**Figure 2. Comparison of OX40L structure**

(A) Phylogenetic analysis of OX40L proteins.

(B) Aminoacid similarity between canine, mouse, and human OX40 ligand.

(C) Aminoacid alignment of OX40L. Extracellular, Transmembrane, and cytoplasmic domains are indicated. Gray boxes highlight the two aminoacid residues, N166 and F180, critical for the interaction of human OX40L with OX40.

recombinant plasmid was used to construct an Expi293-based stable cell line (293F-OX40) expressing cOX40. The cFcOX40L$_B$ selectively binds to canine OX40 on 293F-OX40 cells (Figure 3C),while no binding was observed on the untransfected Expi293 cells (Figure 3D). Taken together, we show that cFcOX40L$_B$ can be produced at high levels, and the recombinant cFcOX40L$_B$ protein binds specifically to cOX40.

## Production and characterization of cFcOX40L$_D$

We also developed a second canine OX40 agonist, cFcOX40L$_D$, by incorporating the Fc region of subclass D of the canine IgG (functional analog of human IgG4). As the Fc region of subclass D of canine IgG has poor binding to protein A, we used the strepTrap column for affinity chromatography, followed by size-exclusion chromatography to achieve high purity of cFcOX40L$_D$(Figures 3E and 3F). SDS-PAGE analysis showed that, like cFcOX40L$_B$, cFcOX40L$_D$ forms dimers under non-denaturing conditions (Figures 3E and 3F). The cFcOX40L$_D$ also selectively binds to canine OX40 on 293F-OX40 cells (Figure 3G), while binding was absent on the untransfected Expi293 cells (Figure 3H). Thus like cFcOX40L$_B$, cFcOX40L$_D$ can be produced at high levels and binds specifically to cOX40.

## Canine OX40 is overexpressed in canine osteosarcomas

After confirming the ability of cFcOX40L proteins to bind cognate cOX40, we used them to investigate the OX40 expression on unstimulated cPBMCs. We observed that cOX40 is not expressed on unstimulated conventional canine CD4$^+$CD3$^+$, CD8$^+$CD3$^+$& CD3$^+$CD4+Foxp3+ regulatory T cells (Figures 4A and S1). We also investigated whether cOX40 is expressed on tumor-infiltrating leukocytes (TILs) in the tumor samples collected from pet dogs with appendicular osteosarcoma (OSA). We analyzed our previously published data from patient-matched primary OSA and normal bone obtained from seven canine osteosarcoma patients (Nance et al., 2022). Following the same bioinformatics pipeline, cOX40 expression was evaluated for differential expression using DEseq2 (v3.14). cOX40 was significantly upregulated in OSA tumors, with a log2 fold-change of 3.11 and an adjusted p-value of $7.16 \times 10^{-6}$. All normal bone

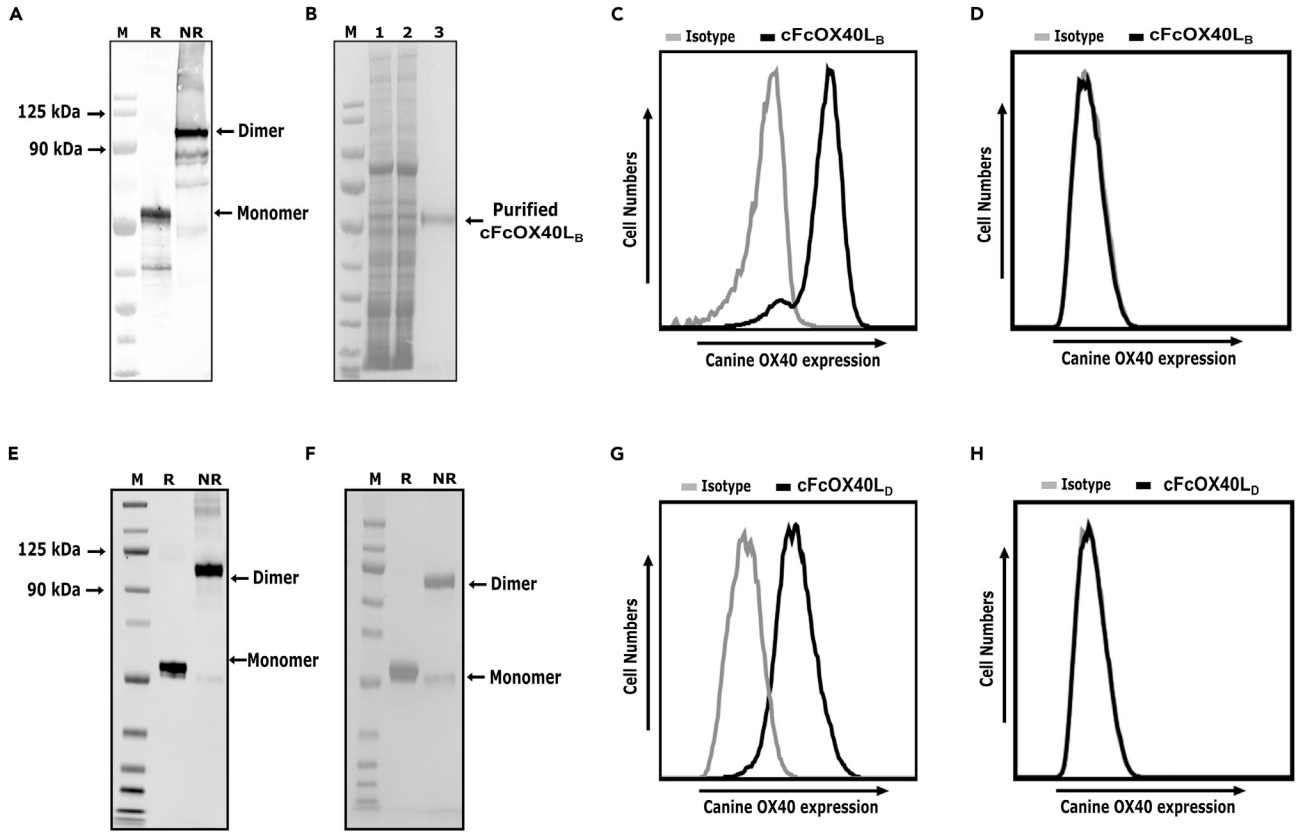


**Figure 3. Development and characterization of cFcOX40L$_B$ and cFcOX40L$_D$**

(A) Expression and purification of cFcOX40L$_B$. Western blot analysis of conditioned media. The cFcOX40L$_B$ was expressed in ExpiCHO-S cells. The conditioned media was resolved under reducing and nonreducing conditions, and the cFcOX40L$_B$ was detected using an anti-IgG Fc antibody. The cFcOX40L$_B$, as expected, forms dimers of ~101 kDa under nonreducing conditions. (R-reducing condition, NR-nonreducing).

(B) Purity of cFcOX40L$_B$ assessed by SDS-PAGE. The cFcOX40L$_B$ was expressed and purified from the ExpiCHO-S cells by affinity (Protein A) and size-exclusion chromatography. The purified cFcOX40L$_B$ was resolved under reducing (R) condition and stained with GelCode Blue Stain.

(C) cFcOX40L$_B$ binds to canine OX40. 293F-OX40 cells were stained with cFcOX40L$_B$, washed, and bound cFcOX40L$_B$ was detected using anti-Fc-750 antibody by flow cytometry.

(D) cFcOX40L$_B$ does not bind to untransfected 293F cells.

(E) Expression and purification of cFcOX40L$_D$. Western blot analysis of conditioned media. The cFcOX40L$_D$ was expressed in ExpiCHO-S cells. The conditioned media was resolved under reducing and nonreducing conditions, and the cFcOX40L$_D$ was detected using an anti-IgG Fc antibody. The cFcOX40L$_D$, as expected, forms dimers of ~101 kDa under nonreducing conditions. (R-reducing condition, NR-nonreducing).

(F) Purity of cFcOX40L$_D$ assessed by SDS-PAGE. The cFcOX40L$_D$ was purified by affinity (StrepTrap HP column) and size-exclusion chromatography. The purified cFcOX40L$_D$ was resolved under reducing (R) and nonreducing (NR) conditions and stained with GelCode Blue Stain.

(G) cFcOX40L$_D$ binds to canine OX40. 293F-OX40 cells were stained with cFcOX40L$_D$, washed, and bound cFcOX40L$_D$ was detected using anti-Fc-DyLight 750 antibody by flow cytometry.

(H) cFcOX40L$_D$ does not bind to untransfected 293F cells.

samples showed negligible expression of cOX40 (Figure 4B). Only one of the seven patients (dog D) showed no change in cOX40 expression in normal bone and tumor.

## Expression profile of OX40 on activated cPBMCs

cPBMCs isolated from three healthy donors were used to characterize the expression profile of cOX40. cOX40 expression is markedly increased on CD3$^+$ T cells after concanavalin A (ConA) stimulation. cOX40 is predominantly expressed on CD4$^+$CD3$^+$T cells(Figures 5A and 5D), and its expression is also detected on a small population of CD8$^+$CD3$^+$T cells (Figures 5B and 5D). Similarly, ConA stimulation also induces OX40 expression on canine CD3$^+$CD4$^+$Foxp3$^+$ regulatory T cells (Tregs) (Figures 5C and 5D). Taken together, we show that cOX40, like hOX40, is not expressed on resting CD3 T cells(Figure S1), while its expression can be induced with ConA. Like hOX40, cOX40 is also expressed on TILs in canine osteosarcoma patients (Figure 4B).

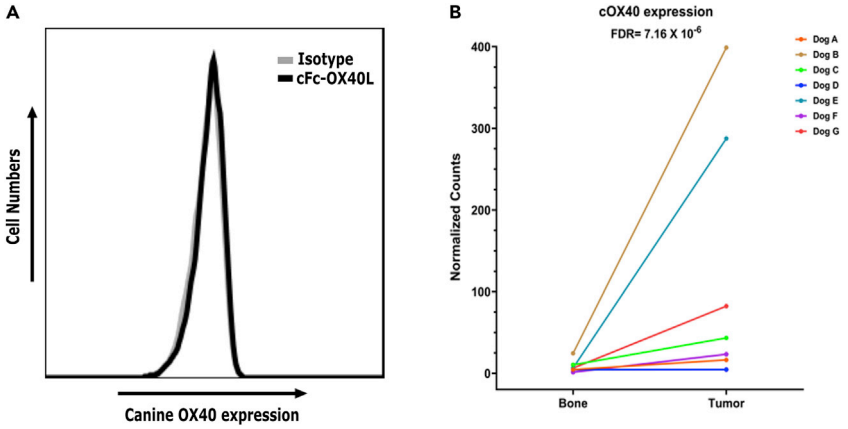


**Figure 4. OX40 is overexpressed in canine osteosarcoma**

(A) Resting cPBMCs do not express OX40. The unstimulated cPBMCs were stained anti-CD4, CD3, CD8, FoxP3, and cFcOX40L and analyzed by flow cytometry. The cOX40 expression was detected using cFcOX40L protein. The OX40 expression was analyzed on various subsets of CD3 T cells. The above histogram shows the lack of cOX40 expression on all $CD3^{+}$T cells.

(B) cOX40 is expressed by TILs in the tumor microenvironment. The differential expression of cOX40 was compared between tumor samples and patient-matched normal bone tissues from seven pet dogs with appendicular osteosarcoma. The plot of the normalized counts of the cOX40 for each dog based on individual-level analysis reveals variation among individual patients. The normalized counts of the cOX40 are shown for each patient. Overall, cOX40 is expressed at significantly higher levels in the tumor tissue compared to patient-matched normal bones, although the differences between tumor and bone are variable between patients. (FDR - False Discovery Rate).

## Canine Fc-OX40L recombinant proteins bind and activate human OX40

As the ECD domain of canine OX40L has a high amino acid similarity to human OX40L, we predicted that $cFcOX40L_B$ and $cFcOX40L_D$ would bind and activate human OX40 signaling. We used a genetically engineered Jurkat T cell-based bioassay to investigate the agonistic activity of $cFcOX40L_B$ and $cFcOX40L_D$. OX40 effector cells in this bioassay express human OX40 and contain a luciferase reporter driven by a response element that can respond to OX40 ligand/agonist antibody stimulation. We first confirmed the binding of $cFcOX40L_B$ and $cFcOX40L_D$ to OX40 effector cells by flow cytometry (Figure 6A). Furthermore, we used OX40 effector cells to prove that $cFcOX40L_B$ and $cFcOX40L_D$ can stimulate a signaling cascade downstream of OX40. The unstimulated OX40 effector cells had a low luminescence signal. The addition of $cFcOX40L_B$ and $cFcOX40L_D$ successfully increased NF-κB promoter activity in a concentration-dependent manner (Figure 6B). There was no increase in the NF-κB promoter activity from OX40 effector cells treated with an isotype control. The EC50 for $cFcOX40L_D$ was 109.5 nM, while the EC50 for $cFcOX40L_B$ was 14.18 nM. Both $cFcOX40L_B$ and $cFcOX40L_D$ did not require Fcγ receptor-mediated cross-linking for OX40 agonism.

## $cFcOX40L_D$ activates cPBMCs

$cFcOX4OL_D$ is not expected to bind to canine Fcγ receptors and mediate Fc receptor-mediated function based on the nature of the parental antibody isotype and also supported by unpublished data. As cOX40, like human OX40, is highly expressed on activated T cells, the depletion of these cells by antibody-dependent cell cytotoxicity (ADCC) will be detrimental to antitumor immunity. Thus, we only examined the ability of the $cFcOX40L_D$ fusion protein to stimulate cPBMCs. We stimulated cPBMCs with ConA (5 μg/mL) in the presence or absence of cFcOX40L and quantified IFN-γ expression at mRNA (TaqMan Assays) and protein levels (ELISA). IFN-γ levels were significantly increased based on mRNA expression (Figure 7A) in the presence of $cFcOX40L_D$ compared to cPBMCs treated with isotype control (polyclonal canine IgG). Increased concentrations of secreted IFN-γ were observed in supernatants of stimulated PBMC, but increases were not statistically significant (Figure 7B). Collectively, we demonstrate that $cFcOX40L_D$ is a potent canine-specific OX40 agonist and can be used to treat canine cancer patients.

## DISCUSSION

Several naturally occurring cancers in pet dogs are well-defined large animal models of human malignancies, including melanoma, pediatric osteosarcoma, glioma, lymphoma, etc. (Simpson

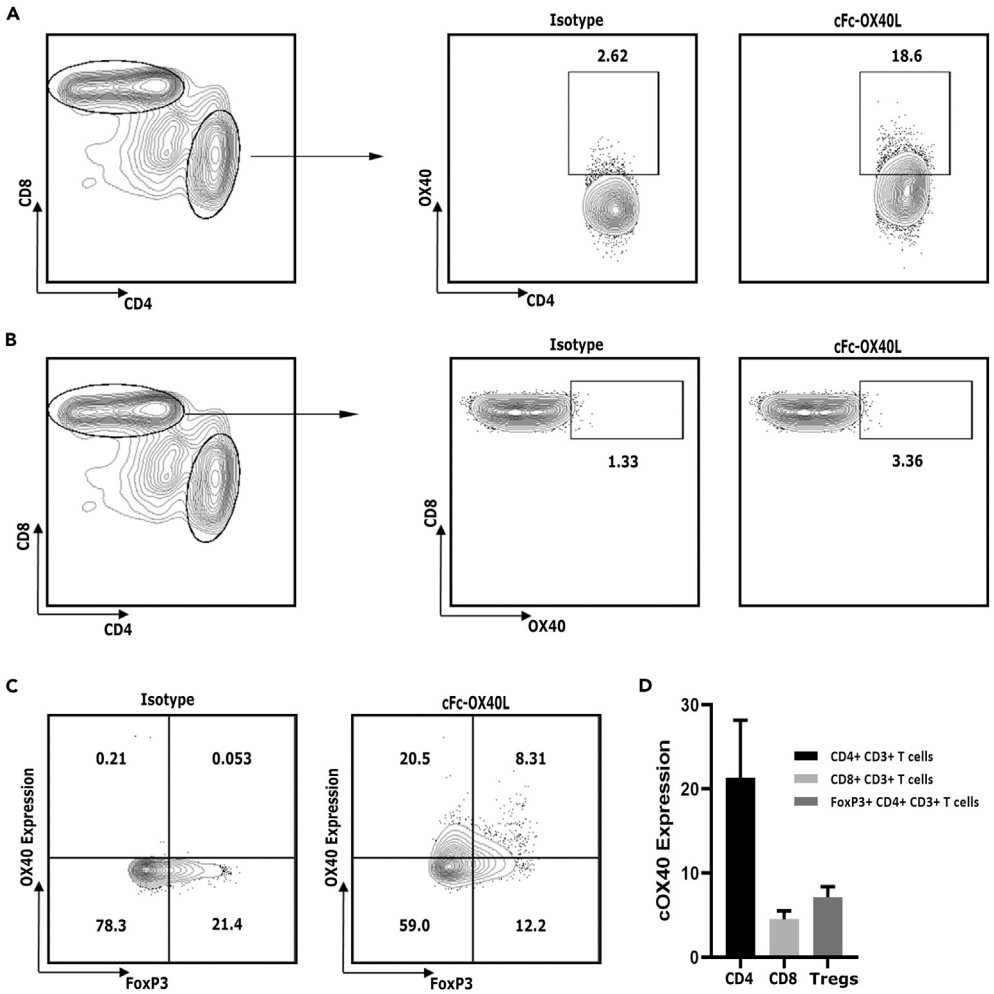


**Figure 5. Activated canine CD3 T cells express OX40**

(A and B) CD4 and CD8 T cells were stimulated with concanavalin A (5 μg/mL) for 72 h. Activated cPBMCs were stained with cFcOX40 $L_B$ fusion protein, and the bound proteins were detected using goat anti-canine IgG Fc DyLight-750 Ab. cPBMCs were also stained with anti-CD3, anti-CD4, and anti-CD8 mAbs. The CD3 T cells were gated to obtain CD4 and CD8 populations, and cOX40 expression was analyzed on these immune subsets by flow cytometry. Canine IgG was used as an isotype control. cOX40 is predominantly expressed on helper T cells, while its expression is restricted to a small population of cytotoxic T cells.

(C) ConA induces OX40 expression on canine Tregs. Activated cPBMCs were similarly stained with anti-CD4CD3, CD8, and cFcOX40$L_B$ fusion protein. The stained cPBMCs were fixed, permeabilized, and treated with anti-FoxP3 eFluor 450 Ab. The $CD4^+CD3^+$T cell population was gated for FoxP3 expression and analyzed for OX40 expression. ConA stimulation induces the expression of cOX40 on cTregs. The binding of cFcOX40$L_B$ to various T-lymphocyte subsets is shown. The cFcOX40$L_D$ also binds similarly to cOX40 on T-lymphocytes (data not shown).

(D) cPBMCs from three healthy dogs were isolated, stimulated with ConA, and analyzed for cOX40 expression. The cOX40 expression on $CD4^+CD3^+$, $CD8^+CD3^+$, and $CD3^+CD4^+FoxP3^+$ T cells from three healthy dogs is shown in the bar graph. Data are represented as mean +/− standard deviation.

et al., 2014; Vail and MacEwen, 2000). Pet dogs develop these cancers spontaneously in the presence of an intact immune system and thus truly mimic the context in which human cancers evolve. Naturally occurring cancers in pet dogs have similar histopathological features, transcriptome/immune profiles, clinical presentation, and response to therapy as their human counterparts (Simpson et al., 2014; Vail and MacEwen, 2000; Palma et al., 2021). However, the lack of canine-specific/cross-reactive immune therapies precludes the utilization of this highly relevant large animal model in immuno-oncology (IO) research.

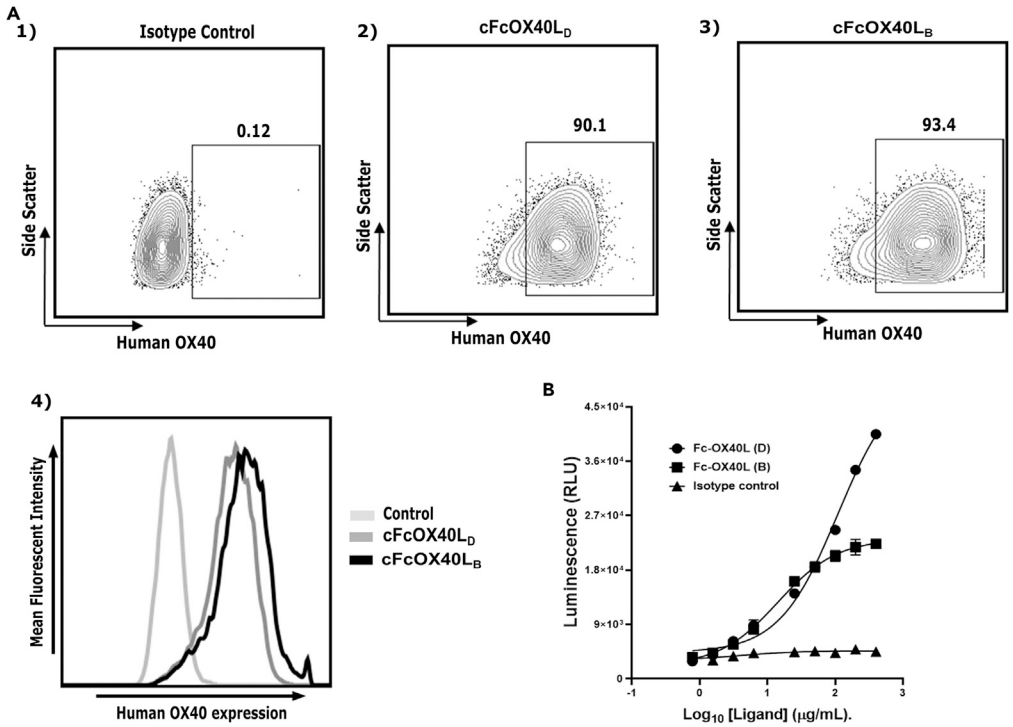


**Figure 6. cFcOX40L$_B$ and cFcOX40L$_D$ bind and activate human OX40**

(A) cFcOX40L$_B$ and cFcOX40L$_D$ bind to human OX40. OX40 effector cells were stained with cFcOX40L$_B$ and cFcOX40L$_D$, and the bound proteins were detected using goat anti-canine IgG Fc DyLight-750 Ab. Both cFcOX40L$_B$ and cFcOX40L$_D$ successfully bind to human OX40 on OX40 effector cells.

(B) cFcOX40L$_B$ and cFcOX40L$_D$ induce NF-κB promotor activity in OX40 effector cells. OX40 effector cells were induced for 5 h with a serial titration of cFcOX40L$_B$, cFcOX40L$_D$, and isotype control (canine IgG Fc). After 5 h of induction, luminescence was detected using Bio-Glo reagent. A three-parameter logistic regression dose-response curve was fit to calculate the EC50 of each recombinant protein.

Herein, we describe the development and characterization of two canine-specific cFcOX40L fusion proteins as an OX40 agonist for canine cancer immunotherapy. We show that cFcOX40Ls, like human Fc-OX40L, are potent OX40 agonists and do not require Fc-receptor-mediated cross-linking for binding and activating OX40 signaling. We show the high aminoacid similarity between human and canine OX40/OX40L proteins compared to mouse orthologs. The ECD of cOX40L protein contains two critical amino acids (F180 and N166), like its human equivalent, vital for hOX40/hOX40L interactions (Compaan and Hymowitz, 2006). The structural similarities between hOX40L/cOX40L were further confirmed by the ability of the cFcOX40L proteins to bind and activate the hOX40 signaling in Jurkat T cell-based bioassay.

We also determine that the expression profile of canine OX40 on various lymphocyte subsets is also very similar to its human counterpart. OX40 is constitutively expressed on the cell surface of murine Tregs and inhibits their suppressive functions (Vu et al., 2007). Conversely, activating signals are requried to induce OX40 expression on human Tregs and conventional T cells (Chen and Flies, 2013). This study shows that the canine OX40, like human OX40, is not expressed on resting conventional T cells. However, its expression rapidly increases after stimulation with activating signals, including concanavalin A and SEB toxin. cOX40, like its human equivalent, is predominantly expressed on activated CD4 T cells as opposed to the activated CD8 T cells (Chen and Flies, 2013). Similarly, resting canine Tregs do not express cOX40. cOX40 is also differentially expressed on the TIL in canine OSA patients compared to patient-matched normal tissues. Thus, we argue that canine OX40-OX40L signaling is more closely related to humans than murine.

In the OX40 bioassay, the cFcOX40L$_D$ showed a different induction profile (EC50, 109.5 vs. 14.18 nM) than cFcOX40L$_B$. However, it is possible that these recombinant proteins will have different induction profiles when tested in canine cells by both *in vitro* assays and canine cancer patients. The cFcOX40L$_D$ and cFcOX40L$_B$ are structurally similar except for the Fc domains derived from the subclass D (functional analog

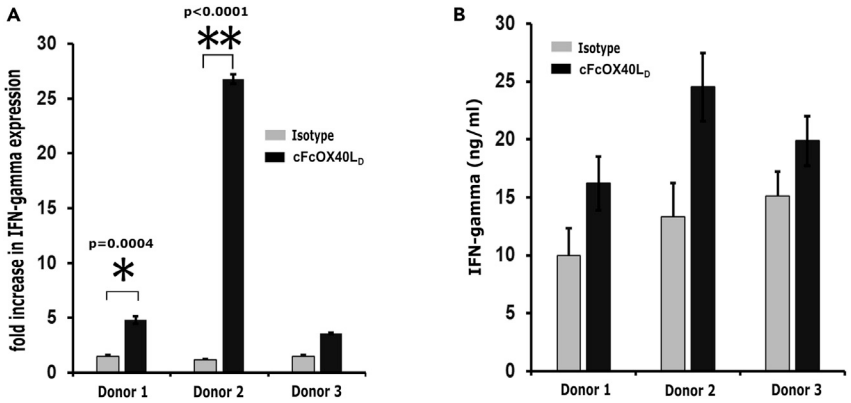


**Figure 7. cFcOX40L$_D$ activates canine PBMCs**

Activated cPBMCs were cultured in the presence or absence of 100 nM of cFcOX40L protein for 72 h.

(A and B) IFN-γ expression was quantified at mRNA and protein levels by TaqMan Assay and ELISA, respectively. Canine IgG was used as the isotype control, while HPRT1 served as an endogenous control for TaqMan Assays. cFcOX40L$_D$ induced activation of cPBMCs and increased IFN-γ expression compared to isotype control. Data are represented as mean ± SEM. p-value of <0.05 was considered statistically significant.

of human IgG4) and B (functional analog of human IgG1) of canine IgG, respectively. Human Fc-OX40L proteins have been previously engineered using the Fc domains of human IgG1 and IgG4 (Morris et al., 2007; Oberst et al., 2018). However, these recombinant proteins (Fc:OX40L and MEDI6383) used different trimerization motifs to attain hexameric structure. The hFc:OX40L, like canine cFcOX40L$_B$, uses the Fc domain of human IgG1, ILZ domain for trimerization and does not require Fc receptor-mediated cross-linking for OX40 activation (Oberst et al., 2018; Morris et al., 2007). MEDI6383 was engineered using the Fc domain of human IgG1 and the ILZ domain from TRAF2 (Oberst et al., 2018). Although it induces OX40 receptor agonism to a limited extent in the solution-phase form, MEDI6383 requires Fc receptor-mediated cross-linking for optimal OX40 activation (Oberst et al., 2018). However, our studies show that cFcOX40L$_D$ and cFcOX40L$_B$, when engineered using the ILZ domain of yeast ICN4, can activate the OX40 receptor in the soluble form and do not require Fcγ mediated cross-linking. In addition, we show that cFcOX40L$_D$ can activate and induce IFN-γ expression from cPBMCs without requiring Fcγ mediated cross-linking.

In conclusion, we found that cFcOX40L$_D$ and cFcOX40L$_B$ are potent activators of OX40 signaling. Thus, these recombinant proteins are attractive candidates to induce durable antitumor immunity and provide novel treatment options for canine cancer patients. Moreover, the availability of these canine-specific IO reagents will allow us to get better insights into their safety, toxicity, pharmacokinetic profile, and antitumor activity in this excellent large animal model of human cancer.

## Limitations of the study

The fusion proteins constructed in this study utilized the coiled-coil trimerization domain derived from yeast GCN4 (ILZ). Thus, canine cancer patients can generate an antibody response against the ILZ domain. The anti-drug antibodies (ADAs) can affect the pharmacokinetic profile or hamper the antitumor activities of anti-OX40 agonists. Thus, we will investigate the ability of other canine-specific trimerization domains, like the TNF receptor-associated factor 2 (TRAF2) coiled-coil domain, in future studies to enable the formation of a covalently linked hexamer.

## STAR★METHODS

Detailed methods are provided in the online version of this paper and include the following:

- KEY RESOURCES TABLE
- RESOURCE AVAILABILITY
  - Lead contact
  - Materials availability
  - Data and code availability
- METHOD DETAILS

- Expression and purification of canine OX40L linked to Fc IgG domain (cFcOX40L)
- Sodium dodecyl sulfate-polyacrylamide gel electrophoresis (SDS-PAGE) and western blotting
- Construction of Expi293F-OX40 cells
- OX40 bioassay
- Differential expression analysis of cOX40
- Purification of canine peripheral blood mononuclear cells (cPBMCs)
- Flow cytometry
- *In vitro* functional assays

- QUANTIFICATION AND STATISTICAL ANALYSIS
  - Statistical analysis

## SUPPLEMENTAL INFORMATION

Supplemental information can be found online at https://doi.org/10.1016/j.isci.2022.105158.

## ACKNOWLEDGMENTS

Authors thank Allison C. Bird (Department of Pathobiology, College of Veterinary Medicine, Auburn University) for performing FACS. This work was funded by the Auburn University Research Initiative in Cancer (AURIC) and the 2021 Research Support Program (AU-RSP).

## AUTHOR CONTRIBUTIONS

The study conception and design were performed by M.S. Data collection and analysis were performed by D.R., C.H., J.M., C.P., P.A., R.L.N., A.S., D.B., A.M., and B.S., D.R. and M.S. wrote the first draft of the manuscript, and all authors commented on previous versions of the manuscript. All authors read and approved the final manuscript.

## DECLARATION OF INTERESTS

The authors declare that they have no competing interests.

## INCLUSION AND DIVERSITY

One or more of the authors of this article self-identifies as an underrepresented ethnic minority in science.

Received: April 25, 2022
Revised: July 19, 2022
Accepted: September 15, 2022
Published: October 21, 2022

## REFERENCES

Adams, V.J., Evans, K.M., Sampson, J., and Wood, J.L.N. (2010). Methods and mortality results of a health survey of purebred dogs in the UK. J. Small Anim. Pract. *51*, 512–524. https://doi.org/10.1111/j.1748-5827.2010.00974.x.

Alsaab, H.O., Sau, S., Alzhrani, R., Tatiparti, K., Bhise, K., Kashaw, S.K., and Iyer, A.K. (2017). PD-1 and PD-L1 checkpoint signaling inhibition for cancer immunotherapy: mechanism, combinations, and clinical outcome. Front. Pharmacol. *8*, 561. https://doi.org/10.3389/fphar.2017.00561.

Bartkowiak, T., and Curran, M.A. (2015). 4-1BB agonists: multi-potent potentiators of tumor immunity. Front. Oncol. *5*, 117. https://doi.org/10.3389/fonc.2015.00117.

Bodmer, J.L., Schneider, P., and Tschopp, J. (2002). The molecular architecture of the TNF superfamily. Trends Biochem. Sci. *27*, 19–26. https://doi.org/10.1016/s0968-0004(01)01995-8.

Buchbinder, E.I., and Desai, A. (2016). CTLA-4 and PD-1 pathways: similarities, differences, and implications of their inhibition. Am. J. Clin. Oncol. *39*, 98–106. https://doi.org/10.1097/coc.0000000000000239.

Burocchi, A., Pittoni, P., Gorzanelli, A., Colombo, M.P., and Piconese, S. (2011). Intratumor OX40 stimulation inhibits IRF1 expression and IL-10 production by Treg cells while enhancing CD40L expression by effector memory T cells. Eur. J. Immunol. *41*, 3615–3626. https://doi.org/10.1002/eji.201141700.

Chan, S., Belmar, N., Ho, S., Rogers, B., Stickler, M., Graham, M., Lee, E., Tran, N., Zhang, D., Gupta, P., et al. (2022). An anti-PD-1-GITR-L bispecific agonist induces GITR clustering-mediated T cell activation for cancer immunotherapy. Nat. Cancer *3*, 337–354. https://doi.org/10.1038/s43018-022-00334-9.

Chen, L., and Flies, D.B. (2013). Molecular mechanisms of T cell co-stimulation and co-inhibition. Nat. Rev. Immunol. *13*, 227–242. https://doi.org/10.1038/nri3405.

Chen, X., Song, X., Li, K., and Zhang, T. (2019). FcγR-binding is an important functional attribute for immune checkpoint Antibodies in cancer immunotherapy. Front. Immunol. *10*, 292. https://doi.org/10.3389/fimmu.2019.00292.

Cloughesy, T.F., Mochizuki, A.Y., Orpilla, J.R., Hugo, W., Lee, A.H., Davidson, T.B., Wang, A.C., Ellingson, B.M., Rytlewski, J.A., Sanders, C.M., et al. (2019). Neoadjuvant anti-PD-1 immunotherapy promotes a survival benefit with intratumoral and systemic immune responses in recurrent glioblastoma. Nat. Med. *25*, 477–486. https://doi.org/10.1038/s41591-018-0337-7.

Compaan, D.M., and Hymowitz, S.G. (2006). The crystal structure of the costimulatory OX40-OX40L complex. Structure *14*, 1321–1330. https://doi.org/10.1016/j.str.2006.06.015.

Croft, M., So, T., Duan, W., and Soroosh, P. (2009). The significance of OX40 and OX40L to T-cell biology and immune disease. Immunol. Rev. *229*, 173–191. https://doi.org/10.1111/j.1600-065X.2009.00766.x.

Diamantopoulos, P., and Gogas, H. (2016). Melanoma immunotherapy dominates the field. Ann. Transl. Med. *4*, 269. https://doi.org/10.21037/atm.2016.06.32.

Duhen, R., Ballesteros-Merino, C., Frye, A.K., Tran, E., Rajamanickam, V., Chang, S.C., Koguchi, Y., Bifulco, C.B., Bernard, B., Leidner, R.S., et al. (2021). Neoadjuvant anti-OX40 (MEDI6469) therapy in patients with head and neck squamous cell carcinoma activates and expands antigen-specific tumor-infiltrating T cells. Nat. Commun. *12*, 1047. https://doi.org/10.1038/s41467-021-21383-1.

Fleming, J.M., Creevy, K.E., and Promislow, D.E. (2011). Mortality in north american dogs from 1984 to 2004: an investigation into age-size-and breed-related causes of death. J. Vet. Intern. Med. *25*, 187–198. https://doi.org/10.1111/j.1939-1676.2011.0695.x.

Gaspal, F.M.C., Kim, M.Y., Mcconnell, F.M., Raykundalia, C., Bekiaris, V., and Lane, P.J.L. (2005). Mice deficient in OX40 and CD30 signals lack memory antibody responses because of deficient CD4 T cell memory. J. Immunol. *174*, 3891–3896. https://doi.org/10.4049/jimmunol.174.7.3891.

Glisson, B.S., Leidner, R.S., Ferris, R.L., Powderly, J., Rizvi, N.A., Keam, B., Schneider, R., Goel, S., Ohr, J.P., Burton, J., et al. (2020). Safety and clinical activity of MEDI0562, ahumanized OX40 agonist monoclonal antibody, in adult patients with advanced solid tumors. Clin. Cancer Res. *26*, 5358–5367. https://doi.org/10.1158/1078-0432.ccr-19-3070.

Gramaglia, I., Jember, A., Pippig, S.D., Weinberg, A.D., Killeen, N., and Croft, M. (2000). The OX40 costimulatory receptor determines the development of CD4 memory by regulating primary clonal expansion. J. Immunol. *165*, 3043–3050. https://doi.org/10.4049/jimmunol.165.6.3043.

Gramaglia, I., Weinberg, A.D., Lemon, M., and Croft, M. (1998). Ox-40 ligand: a potent costimulatory molecule for sustaining primary CD4 T cell responses. J. Immunol. *161*, 6510–6517.

Guo, Z., Wang, X., Cheng, D., Xia, Z., Luan, M., and Zhang, S. (2014). PD-1 blockade and OX40 triggering synergistically protects against tumor growth in a murine model of ovarian cancer. PLoS One *9*, e89350. https://doi.org/10.1371/journal.pone.0089350.

Gutierrez, M., Moreno, V., Heinhuis, K.M., Olszanski, A.J., Spreafico, A., Ong, M., Chu, Q., Carvajal, R.D., Trigo, J., Ochoa De Olza, M., et al. (2021). OX40 agonist BMS-986178 alone or in combination with nivolumab and/or ipilimumab in patients with advanced solid tumors. Clin. Cancer Res. *27*, 460–472. https://doi.org/10.1158/1078-0432.ccr-20-1830.

Hirschhorn-Cymerman, D., Budhu, S., Kitano, S., Liu, C., Zhao, F., Zhong, H., Lesokhin, A.M., Avogadri-Connors, F., Yuan, J., Li, Y., et al. (2012). Induction of tumoricidal function in CD4+ T cells is associated with concomitant memory and terminally differentiated phenotype. J. Exp. Med. *209*, 2113–2126. https://doi.org/10.1084/jem.20120532.

Huddleston, C.A., Weinberg, A.D., and Parker, D.C. (2006). OX40 (CD134) engagement drives differentiation of CD4+ T cells to effector cells. Eur. J. Immunol. *36*, 1093–1103. https://doi.org/10.1002/eji.200535637.

Igase, M., Nemoto, Y., Itamoto, K., Tani, K., Nakaichi, M., Sakurai, M., Sakai, Y., Noguchi, S., Kato, M., Tsukui, T., and Mizuno, T. (2020). A pilot clinical study of the therapeutic antibody against canine PD-1 for advanced spontaneous cancers in dogs. Sci. Rep. *10*, 18311. https://doi.org/10.1038/s41598-020-75533-4.

Kopf, M., Ruedl, C., Schmitz, N., Gallimore, A., Lefrang, K., Ecabert, B., Odermatt, B., and Bachmann, M.F. (1999). OX40-deficient mice are defective in Th cell proliferation but are competent in generating B cell and CTL Responses after virus infection. Immunity *11*, 699–708. https://doi.org/10.1016/s1074-7613(00)80144-2.

Lee, S.J., Myers, L., Muralimohan, G., Dai, J., Qiao, Y., Li, Z., Mittler, R.S., and Vella, A.T. (2004). 4-1BB and OX40 dual costimulation synergistically stimulate primary specific CD8 T cells for robust effector function. J. Immunol. *173*, 3002–3012. https://doi.org/10.4049/jimmunol.173.5.3002.

Marable, J., Ruiz, D., Jaiswal, A.K., Bhattacharya, R., Pantazes, R., Agarwal, P., Suryawanshi, A.S., Bedi, D., Mishra, A., Smith, B.F., and Sandey, M. (2021). Nanobody-based CTLA4 inhibitors for immune checkpoint blockade therapy of canine cancer patients. Sci. Rep. *11*, 20763. https://doi.org/10.1038/s41598-021-00325-3.

Mason, N.J., Chester, N., Xiong, A., Rotolo, A., Wu, Y., Yoshimoto, S., Glassman, P., Gulendran, G., and Siegel, D.L. (2021). Development of a fully canine anti-canine CTLA4 monoclonal antibody for comparative translational research in dogs with spontaneous tumors. mAbs *13*, 2004638. https://doi.org/10.1080/19420862.2021.2004638.

Mayes, P.A., Hance, K.W., and Hoos, A. (2018). The promise and challenges of immune agonist antibody development in cancer. Nat. Rev. Drug Discov. *17*, 509–527. https://doi.org/10.1038/nrd.2018.75.

Melero, I., Hirschhorn-Cymerman, D., Morales-Kastresana, A., Sanmamed, M.F., and Wolchok, J.D. (2013). Agonist antibodies to TNFR molecules that costimulate T and NK cells. Clin. Cancer Res. *19*, 1044–1053. https://doi.org/10.1158/1078-0432.ccr-12-2065.

Morris, N.P., Peters, C., Montler, R., Hu, H.M., Curti, B.D., Urba, W.J., and Weinberg, A.D. (2007). Development and Characterization of Recombinant Human Fc:OX40L fusion protein linked via a coiled-coil trimerization domain. Mol. Immunol. *44*, 3112–3121. https://doi.org/10.1016/j.molimm.2007.02.004.

Murata, S., Ladle, B.H., Kim, P.S., Lutz, E.R., Wolpoe, M.E., Ivie, S.E., Smith, H.M., Armstrong, T.D., Emens, L.A., Jaffee, E.M., and Reilly, R.T. (2006). OX40 costimulation synergizes with GM-CSF whole-cell vaccination to overcome established CD8+ T cell tolerance to an endogenous tumor antigen. J. Immunol. *176*, 974–983. https://doi.org/10.4049/jimmunol.176.2.974.

Murphy, K.A., Erickson, J.R., Johnson, C.S., Seiler, C.E., Bedi, J., Hu, P., Pluhar, G.E., Epstein, A.L., and Ohlfest, J.R. (2014). CD8+ T cell-independent tumor regression induced by Fc-OX40L and therapeutic vaccination in a mouse model of glioma. J. Immunol. *192*, 224–233. https://doi.org/10.4049/jimmunol.1301633.

Nance, R.L.C., Cooper, S.J., Starenki, D., Wang, X., Matz, B., Lindley, S., Smith, A.N., Smith, A.A., Bergman, N., et al. (2022). Transcriptomic analysis of canine osteosarcoma from a precision medicine perspective reveals limitations of differential geneexpression studies. Genes *13*, 680. https://doi.org/10.3390/genes13040680.

Oberst, M.D., Augé, C., Morris, C., Kentner, S., Mulgrew, K., Mcglinchey, K., Hair, J., Hanabuchi, S., Du, Q., Damschroder, M., et al. (2018). Potent immune modulation by MEDI6383, an engineered human OX40 ligand IgG4P Fc fusion protein. Mol. Cancer Ther. *17*, 1024–1038. https://doi.org/10.1158/1535-7163.mct-17-0200.

Palma, S.D., Mcconnell, A., Verganti, S., and Starkey, M. (2021). Review on canine oral melanoma: anundervalued authentic genetic model of human oral melanoma? Vet. Pathol. *58*, 881–889. https://doi.org/10.1177/0300985821996658.

Pardee, A.D., Mccurry, D., Alber, S., Hu, P., Epstein, A.L., and Storkus, W.J. (2010). A therapeutic OX40 agonist dynamically alters dendritic, endothelial, and T cell subsets within the established tumor microenvironment. Cancer Res. *70*, 9041–9052. https://doi.org/10.1158/0008-5472.CAN-10-1369.

Piconese, S., Valzasina, B., and Colombo, M.P. (2008). OX40 triggering blocks suppression by regulatory T cells and facilitates tumor rejection. J. Exp. Med. *205*, 1505–1839. https://doi.org/10.1084/jem.20071341051208c.

Redmond, W.L., Linch, S.N., and Kasiewicz, M.J. (2014). Combined targeting of costimulatory (OX40) and coinhibitory (CTLA-4) pathways elicits potent effector T cells capable of driving robust antitumor immunity. Cancer Immunol. Res. *2*, 142–153. https://doi.org/10.1158/2326-6066.cir-13-0031-t.

Redmond, W.L., Ruby, C.E., and Weinberg, A.D. (2009). The role of OX40-mediated co-stimulation in T-cell activation and survival. Crit. Rev. Immunol. *29*, 187–201. https://doi.org/10.1615/critrevimmunol.v29.i3.10.

Rogers, P.R., Song, J., Gramaglia, I., Killeen, N., and Croft, M. (2001). OX40 promotes Bcl-xL and Bcl-2 expression and is essential for long-term survival of CD4 T cells. Immunity *15*, 445–455. https://doi.org/10.1016/s1074-7613(01)00191-1.

Simpson, R.M., Bastian, B.C., Michael, H.T., Webster, J.D., Prasad, M.L., Conway, C.M., Prieto, V.M., Gary, J.M., Goldschmidt, M.H., Esplin, D.G., et al. (2014). Sporadic naturally occurring melanoma in dogs as a preclinical model for human melanoma. Pigment Cell Melanoma Res. *27*, 37–47. https://doi.org/10.1111/pcmr.12185.

Smith, S.E., Hoelzinger, D.B., Dominguez, A.L., Van Snick, J., and Lustgarten, J. (2011). Signals through 4-1BB inhibit T regulatory cells by blocking IL-9 production enhancing antitumor responses. Cancer Immunol.Immunother. *60*, 1775–1787. https://doi.org/10.1007/s00262-011-1075-6.

Song, J., So, T., Cheng, M., Tang, X., and Croft, M. (2005). Sustained survivin expression from OX40 costimulatory signals drives T cell clonal expansion. Immunity *22*, 621–631. https://doi.org/10.1016/j.immuni.2005.03.012.

Vail, D.M., and MacEwen, E.G. (2000). Spontaneously occurring tumors of companion animals as models for human cancer. Cancer Invest. *18*, 781–792. https://doi.org/10.3109/07357900009012210.

Vanamee, É.S., and Faustman, D.L. (2018). Structural principles of tumor necrosis factor superfamily signaling. Sci. Signal. *11*. https://doi.org/10.1126/scisignal.aao4910.

Vu, M.D., Xiao, X., Gao, W., Degauque, N., Chen, M., Kroemer, A., Killeen, N., Ishii, N., and Chang Li, X. (2007). OX40 costimulation turns off Foxp3+ Tregs. Blood *110*, 2501–2510. https://doi.org/10.1182/blood-2007-01-070748.

Wolchok, J.D., Kluger, H., Callahan, M.K., Postow, M.A., Rizvi, N.A., Lesokhin, A.M., Segal, N.H., Ariyan, C.E., Gordon, R.A., Reed, K., et al. (2013). Nivolumab plus ipilimumab in advanced melanoma. N. Engl. J. Med. *369*, 122–133. https://doi.org/10.1056/NEJMoa1302369.

## STAR★METHODS

### KEY RESOURCES TABLE

| REAGENT or RESOURCE | SOURCE | IDENTIFIER |
|---|---|---|
| **Antibodies** | | |
| Rabbit anti-canine IgG Fc | Novus Biologicals | Cat# NBP1-72773; RRID:AB_11011451 |
| Mouse anti-Strep Tag II | Novus Biologicals | Cat# NBP2-43735; RRID:AB_2916323 |
| IRDye680RD Donkey anti-Mouse | LI-COR | Cat# 926-68072; RRID:AB_10953628 |
| IRDye680RD Donkey anti-Rabbit | LI-COR | Cat# 926-68073; RRID:AB_10954442 |
| Goat anti-canine IgG Fc DyLight 750 | Novus Biologicals | Cat# NBP1-72772IR; RRID:AB_11034363 |
| anti-CD3FITC | BIO-RAD | Clone CA17.2A12; RRID:AB_2528916 |
| anti-CD4RPE | BIO-RAD | Clone YKIX 302.9; RRID:AB_2528939 |
| anti-CD8 AF 647 | BIO-RAD | Clone YCATE55.9; RRID:AB_2529097 |
| Anti-FoxP3 eFluor 450 | ThermoFisher Scientific | Clone FJK-16s; RRID:AB_1518813 |
| Anti-CD3 mAb | Dr. Peter Moore | CA17.6F9 |
| Canine IgG Isotype Control | Novus Biologicals | Cat# NBP1-97051 |
| **Biological samples** | | |
| Canine appendicular osteosarcoma (OSA) tumor cells | Auburn University College of Veterinary Medicine | N/A |
| Canine peripheral blood mononuclear cells (cPBMCs) | Auburn University College of Veterinary Medicine | N/A |
| Fetal Bovine Serum (FBS) | Peak Serum | Cat# PS-FB4 |
| **Chemicals, peptides, and recombinant proteins** | | |
| Desethiobiotin | Millipore Corp | Cat# 71610 |
| Concanavalin A | ThermoFisher Scientific | Cat# J61221-MC |
| Recombinant IL-2 | R&D systems | Cat# 1815-CL-020/CF |
| Gibco 1X MEM nonessential amino acids (NEAA) | ThermoFisher Scientific | Cat# 11140-050 |
| Gibco Sodium Pyruvate | ThermoFisher Scientific | Cat# 11360-070 |
| DMEM Media | Cytiva Life Sciences | Cat# SH30243.01 |
| RPMI Media | Cytiva Life Sciences | Cat# SH30255.01 |
| Dulbecco's PBS (DPBS) | Cytiva Life Sciences | Cat# SH30028.02 |
| Histopaque-1077 | Sigma-Aldrich | Cat# 10771 |
| **Critical commercial assays** | | |
| ExpiFectamine CHO transfection kit | ThermoFisher Scientific | Cat# A29130 |
| Slide-A-Lyzer dialysis cassette | ThermoFisher Scientific | Cat# 87726 |
| HiTrap Protein A HP column | GE Healthcare | Cat# 29-048-76 |
| StrepTrap column | Cytiva Life Sciences | Cat# 29048653 |
| Pierce 30 kDa MWCO protein concentrators | ThermoFisher Scientific | Cat# 88529 |
| GelCode Blue Safe Protein Stain | ThermoFisher Scientific | Cat# 24594 |
| Lipofectamine 3000 | ThermoFisher Scientific | Cat# L3000015 |
| Canine IFN-γ ELISA kit | R&D Systems | Cat# DY781B |
| Bio-Glo Luciferase Assay System | Promega | Cat# G7941 |
| Sepmate PBMC isolation tubes | StemCell Technologies | Cat# 15450 |
| FIX & PERM Cell Fixation & Cell Permeabilization Kit | ThermoFisher Scientific | Cat# GAS003 |
| Canine IFN-γ TaqMan assay | ThermoFisher Scientific | Cat# Cf02623316_m1 |
| Canine HPRT1 TaqMan Assay | ThermoFisher Scientific | Cat# Cf02690456_g1 |

(*Continued on next page*)

*Continued*

| REAGENT or RESOURCE | SOURCE | IDENTIFIER |
|---|---|---|
| Deposited data | | |
| RNA Sequencing Data | NCBI GEO database | Accession ID: GSE199489 |
| Recombinant DNA | | |
| pCDNA3.1/Hygro$^{(+)}$ | ThermoFisher Scientific | Cat# V87020 |
| Experimental models: Cell lines | | |
| ExpiCHO-S cells | ThermoFisher Scientific | Cat# A29127 |
| Expi293F cells | ThermoFisher Scientific | Cat# A14527 |
| OX40 effector cells (OX40 Bioassay) | Promega | Cat# JA2191 |
| Software and algorithms | | |
| SAS/STAT software | SAS Institute | http://www.sas.com |
| FlowJo_v10.8.1 | BD Biosciences | https://www.flowjo.com |

## RESOURCE AVAILABILITY

### Lead contact

Information and requests for resources should be directed to and will be fulfilled by the corresponding author, Maninder Sandey (mzs0011@auburn.edu).

### Materials availability

All recombinant plasmids generated in this study have the potential for commercial development to treat canine cancer patients. These tools will be shared following typical intellectual property agreements. All other reagents were purchased commercially from the vendors described in the key resources table.

### Data and code availability

- RNA-seq data have been deposited at GEO and are publicly available as of the date of publication. Accession number is GSE199489.
- All other data generated or analyzed during this study are included in this published article. All other data reported in this article will be shared by the lead contacton request.
- This article does not report original code.

## METHOD DETAILS

All animal procedures, including collecting blood samples from healthy donors (colony animals), were reviewed and approved by the Auburn University Institutional Animal Care and Use Committee (IACUC). All methods are reported in accordance with ARRIVE guidelines for the reporting of animal experiments. All procedures were performed by following the relevant guidelines and regulations.

### Expression and purification of canine OX40L linked to Fc IgG domain (cFcOX40L)

The nucleotide sequence coding for canine OX40L was fused *in silico* to the Fc domain of subclass B (functional analog of human IgG1) or D (functional analog of human IgG4) of canine IgG via coiled-coil trimerization domain derived from yeast GCN4 (ILZ). We placed a secretion signal sequence from the V-J2-C region of the mouse Ig Kappa-chain at the N-terminus for efficient secretion of the cFcOX40L proteins after transient transfection. A strep Tag II was placed immediately after the secretion signal to purify these proteins by affinity chromatography. The DNA sequences coding for the cFcOX40L$_B$ and cFcOX40L$_D$ were synthesized and cloned into a mammalian expression vector pCDNA3.1/Hygro$^{(+)}$. The recombinant plasmids were transiently transfected into ExpiCHO-S cells using the ExpiFectamine CHO transfection kit (Thermo Fisher). Seven days after transfection, the ExpiCHO-S cells and conditioned media were harvested for protein purification. The ExpiCHO-S cells were separated from the conditioned media by centrifugation at 4000*g* for 30 min at 4°C. The supernatant containing the cFcOX40L$_B$ protein was collected and dialyzed against 1X HiTrap Protein A buffer (20 mM Sodium Phosphate, pH 7.0) for 2 h at room temperature in a Slide-A-Lyzer dialysis cassette (Thermo Scientific). Following the initial 2 h, the dialysis buffer was

exchanged with fresh buffer, and the proteins were dialyzed under the same conditions for another 2 h. The dialysis buffer was exchanged for the third time, and the conditioned media was dialyzed overnight at 4°C. The conditioned media was centrifuged for 10 min at 10,000g (4°C) to remove any precipitated proteins from the overnight dialyzed sample. The HiTrap Protein A HP column was equilibrated using 10 column volumes of wash buffer (10 mM sodium phosphate [pH 7.0]). The dialyzed conditioned media was applied to the equilibrated column using AKTA explorer. The bound protein was eluted with 100 mM sodium citrate (pH 3.0) directly into 1M Tris-Hcl (pH 9; 0.25 mL/mL elution). As cFcOX40L$_D$ protein has a low affinity to Protein A, we use a StrepTrap column to purify it from the conditioned media using a similar protocol (Cytiva Life Sciences). The bound protein was eluted with the elution buffer (100 mM Tris-HCl, 150 mM NaCl & 1 mM EDTA) containing 2.5 mM desthiobiotin. Finally, the purified recombinant proteins were diluted into 1X PBS and concentrated using 30 kDa protein concentrators (Pierce™). Purified proteins were filter-sterilized (0.2 μM), snap-frozen in liquid nitrogen, and stored at −80°C.

### Sodium dodecyl sulfate-polyacrylamide gel electrophoresis (SDS-PAGE) and western blotting

The expression of recombinant proteins was initially validated by western blot analysis. The conditioned media containing the recombinant proteins was resolved under reducing (beta-mercaptoethanol) and nonreducing conditions and transferred to the nitrocellulose membrane. Rabbit anti-canine IgG Fc antibodies (Novus Biologicals) and anti-Strep Tag II antibodies were used to detect recombinant proteins. Secondary antibodies conjugated with IRDye680RD (LI-COR Biosciences) were used to detect the primary antibodies, and the blots were scanned on LI-COR Odyssey 9120 digital scanning system. To confirm the purity, 1.0 μg of recombinant proteins were resolved under reducing and nonreducing conditions by SDS-PAGE. The gel was stained with GelCode Blue Safe Protein Stain (Thermo Fisher Scientific).

### Construction of Expi293F-OX40 cells

The open reading frame (ORF) coding for canine OX40 was amplified and cloned in the pCDNA3.1/Hygro$^{(+)}$ vector. The recombinant plasmid was confirmed by sequencing and used to generate stable cell lines expressing canine OX40. Briefly, Lipofectamine 3000 (Life Technologies) was used to transfect Expi293F cells with recombinant plasmids expressing canine OX40. The transfected Expi293F cells were treated with hygromycin and sorted by flow cytometry to obtain single-cell clones. Expi293F cells that stably expressed OX40 (293F-OX40) were maintained in DMEM media supplemented with 10% fetal bovine serum (FBS) at 37% in 5% $CO_2$.

### OX40 bioassay

The Promega OX40 bioassay kit was used to determine the functional activity of cFcOX40L$_B$ and cFcOX40L$_D$. OX40 effector cells (Promega, Inc) were maintained and propagated in Roswell Park Memorial Institute (RPMI) 1640 medium supplemented with 10% fetal bovine serum (FBS), 1X MEM nonessential amino acids (NEAA), and 1 mM sodium pyruvate. The OX40 effector cells were maintained between 0.8–1.5 × $10^6$ cells/mL. The culture conditions were optimized to keep the cell viability greater than 90%. Recombinant proteins were serially diluted (400–1.25 nM) in assay buffer, and 25 μL of the diluted recombinant proteins and isotype control were added to the assay plate in duplicates. OX40 effector cells with cell viability greater than 90% were collected at 130 × g for 10 min at ambient temperature. The cell pellet was resuspended in assay buffer to generate the targeted cell density of 1.0 × $10^6$ cells/mL. Using a multichannel pipette, 50μL (0.5 × $10^5$ cells) of OX40 Effector cells were dispensed into wells containing different dilutions of recombinant proteins and an isotype control. The assay plate was covered with a lid and incubated in a 37°C, 5% CO2 incubator for 5 h. After 5 h, the assay plate was removed from the incubator and equilibrated to ambient temperature for 10 min. Using a manual multichannel pipette, 75μL of Bio-GloReagent was added to all wells. The assay plate was incubated at room temperature for 5 min, and luminescence was measured using a Tecan M2000 plate reader. The average relative luminescence unit (RLU) was calculated for each dilution. The average RLU data were plotted against the different concentrations of cFcOX40L proteins and an isotype control. A three-parameter logistic regression dose-response curve was fit to calculate EC50 (the concentration of agonist that gives a response halfway between bottom and top) of each recombinant protein.

### Differential expression analysis of cOX40

We analyzed our previously published RNA sequencing data collected from seven pet dogs with appendicular osteosarcoma (OSA) at the Auburn University College of Veterinary Medicine in Auburn, AL (GSE199489). Briefly, tumor samples and patient-matched normal bones were used to prepare RNA sequencing libraries (Nance et al., 2022). Following the same bioinformatics pipeline as previously described (Nance et al., 2022), we evaluated the differential expression of cOX40 in tumor samples and patient-matched normal bones using DEseq2 (v3.14).

### Purification of canine peripheral blood mononuclear cells (cPBMCs)

cPBMCs were isolated from the peripheral blood using the published protocol (Marable et al., 2021). Briefly, peripheral blood collected from three healthy dogs was diluted 1:1 with Dulbecco's phosphate buffer saline (DPBS). Two SepMate PBMC isolation tubes were filled with 15 mL of Histopaque-1077 (Sigma). The diluted blood sample was carefully layered over the SepMate insert. The layered blood was centrifuged at 800 x g for 10 min. The PBMCs layer was carefully collected and diluted with DPBS in a new 15 mL conical tube. The cell suspension was mixed well and centrifuged at 800 x g for 10 min. The supernatant was discarded, and the cell pellet was resuspended and rewashed with DPBS. After the supernatant was discarded, the cells were resuspended in complete RPMI-1640 media containing 10% fetal bovine serum (FBS) plus penicillin (200 U/mL) and streptomycin (100 μg/mL). The cPBMCs were cultured overnight in flasks, and non-adherent cells were gently collected and used for various experiments. Cells were stained after overnight resting incubation to evaluate cOX40 expression on unstimulated cPBMC.

### Flow cytometry

Expi293 and 293F-OX40 cells were trypsinized and washed with FACS buffer (1X PBS containing 1% BSA, 2 mM EDTA, 0.02% sodium azide, and HEPES). Cells were incubated in blocking buffer (PBS containing 4% goat or rabbit serum, 1% BSA, 0.02% sodium azide) and stained with recombinant proteins and isotype control (canine IgG). Bound recombinant proteins were detected with anti-canine IgG Fc DyLight 750 secondary antibody and analyzed by flow cytometry. Canine PBMC were cultured overnight in RPMI media. PBMCs were stimulated with concanavalin A (ConA; 5 μg/mL final concentration) for 72 h. Stimulated PBMCs were blocked and stained with 100 nM of recombinant proteins. Cells were also stained with anti-CD3FITC (clone CA17.2A12, Bio-Rad), anti-CD4RPE (clone YKIX 302.9, Bio-Rad), and anti-CD8AF 647 (clone YCATE55.9, Bio-Rad) antibodies. 5 μL of antibody cocktail containing anti-$CD4^+CD3^+$ and CD8 mAbs was used to stain 300,000 cells. For intracellular FoxP3 staining, cells were first stained for surface markers and then fixed and permeabilized using the fix and perm cell permeabilization kit from Life Technologies. Cells were then stained with anti-FoxP3 eFluor 450 monoclonal antibody (Thermo Fisher). 50,000 cells were analyzed on a Beckman Coulter CytoFlex S flow cytometer. Flow cytometry data were analyzed with FlowJo_v10.8.1 (BD Biosciences).

### *In vitro* functional assays

All animal procedures, including the collection of blood samples from healthy dogs, were reviewed and approved by the Auburn University IACUC. cPBMCs isolated from three healthy dogs were stimulated with ConA (5 μg/mL) and IL-2 for 48 h. The activated PBMCs were then incubated with 100 nM of $cFcOX40L_D$ protein and suboptimal levels (1 μg/mL) of anti-CD3 antibody as previously described (Oberst et al., 2018). Canine IgG was used as isotype control. After three days of incubation with $cFcOX40L_D$, the supernatant was collected, and IFN-γ was measured by the Canine IFN-γ ELISA kit (R&D system). Similarly, RNA was isolated from stimulated PBMCs, reverse-transcribed, and quantified for IFN-γ mRNA levels using TaqMan assays (cf.02623316_m1) as previously described (Marable et al., 2021). All assays were performed in triplicates, and HPRT1 (cf.02690456_g1) was used as endogenous control.

## QUANTIFICATION AND STATISTICAL ANALYSIS

### Statistical analysis

All assays were performed in triplicates, and the collected data were compared using a two-sample t-test. All statistical analysis was performed with SAS/STAT software (SAS Institute, Inc.). All statistical tests were two-sided, and a p-value of $<0.05$ was regarded as statically significant.